Available online at www.jourcc.com

Journal homepage: www.JOURCC.com

Journal of Composites and Compounds

Investigation of aluminum oxide coatings created by electrolytic plasma method in different potential regimes

*Mahsa Amiri[a], Saman Padervand [a], Vahid Tavakoli Targhi [a], Seyed Mohammad Mousavi khoei [a]**

[a] *Material and Metallurgical Engineering Department, Amirkabir University of Technology, Hafez Street, Tehran, Iran*

ABSTRACT

One of the most important coating methods on aluminum surfaces is the electrolytic plasma method. The main objective of the present study is to investigate the potential of aluminum oxide coatings created by electrolytic plasma method. Aluminum series 2 and the electrolyte of sodium silicate, sodium tetraphosphate, sodium aluminate, and potassium hydroxide were used. The results showed that the appropriate voltage to achieve uniform coating with ideal thickness and morphology is 500 V. Adding sodium silicate to the electrolyte solution will create porosity and non-adhesion to the substrate. On the other hand, the use of tetra sodium pyrophosphate increases the adhesion of the coating by penetrating phosphorus into the metal/coating interface. The optimum solution for plasma electrolytic oxidation coatings composed of 10, 3, and 3 g/l of tetra sodium pyrophosphate, sodium aluminate, and KOH, respectively. DC pulsed coating was shown to control the coating process and coating uniformity. Also the appropriate frequency to apply coating was DC pulse potential at 1000 Hz frequency under the 30% duty cycle.

Peer review under responsibility of JCC Research Group

ARTICLE INFORMATION

Article history:
Received 05 June 2020
Received in revised form 23 July 2020
Accepted 16 September 2020

Keywords:
Electrolyte plasma method
Aluminum oxide coatings
Potential applied regime

1. Introduction

Nowadays, many efforts have been made to expand the application of aluminum, its alloys and its composites [1-4]. In this regard, surface optimization of Al and its alloys by using easy, low-cost, and environmentally friendly methods is one of the most important fields of research [5-7]. Most surface engineering methods used in this regard are either costly (such as CVD methods, gas plasma, hot-dipping, and all vacuum-based methods) or they cause environmental problems (viz. anodizing methods or surface conversion coatings like chromate coatings) [8-11]. The oxidation method, unlike anodizing methods, is an eco-friendly method due to the use of alkaline solutions. In addition, by using the plasma electrolytic oxidation (PEO) method, creating thicker and more continuous coatings on the aluminum surface is possible [12-15]. PEO is a low-cost method among surface engineering techniques due to the creation of plasma in the electrolyte environment without requiring special conditions such as a vacuum or high temperature, and the use of simple and inexpensive salts [16]. By using the electric discharge and an electric arc generation at the metal/solution interface, it is possible to apply coatings with various properties and structures by controlling the electrical and electrolytic parameters. These advantages have attracted attention in industrial applications [17]. Coating of aluminum as well as its composites, and the deposition of hybrid and composite coatings on aluminum can be conducted by the PEO method.

PEO is a process for the chemical conversion of a metal surface into a hard oxide coating [18]. Aluminum is widely used in the aerospace and automotive industries due to its properties such as high corrosion resistance and high strength to weight ratio. However, the short-comings such as low hardness, low wear resistance and also high friction coefficient, have limited the use of aluminum alloys [19]. When the PEO layer is applied on the surface of aluminum, Al_2O_3 coating is formed on the surface of the sample, which causes good performance [20], high thermal resistance [21] , and good dielectric properties in the sample [22, 23]

Al_2O_3 compound is chemically stable and its melting temperature is as high as 2054 °C [24-27]. Therefore, it can be used in high temperature applications. Due to high hardness, strength and abrasion resistance of Al_2O_3, this material is offered as a promising material for catalysts and biological implantation [28, 29].

Recent research in the field of PEO coatings has focused on controlling the structure and morphology, stress level control, and the reduction of crack networks. In this research, the coating defects including porosity and crack networks are controlled by adjusting the electrical parameters to obtain improved properties for PEO aluminum coatings.

2. Materials and methods

2.1. Materials

In this research, 2025 aluminum sheet with a thickness of 4 mm, made by Arak Rolling Co, Iran, was used. The Al alloy contained 0.23% Si, 0.6% Fe, 0.22% Mg, 0.11% St, and 0.03 % Sn. Aluminum specimens with dimensions of 4×20×20 mm were cut. The surfaces of the samples were sanded with silicon carbide sandpapers up to the grit number of

* *Corresponding author: Seyed Mohammad Mousavi khoei; E-mail:* Mmousavi@aut.ac.ir

DOR: 20.1001.1.26765837.2020.2.4.2.4
https://doi.org/10.29252/jcc.2.3.2

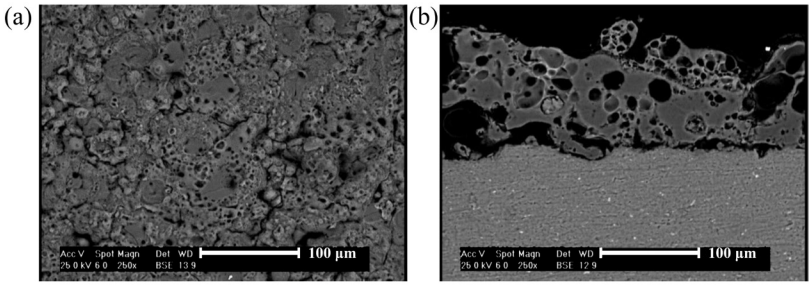

Fig. 1. SEM image of (a) surface and (b) cross-sectional area of sample 1 coated in electrolyte solution containing 2.5 g/l potash, 10 g/l sodium silicate under 500 V and 10 min.

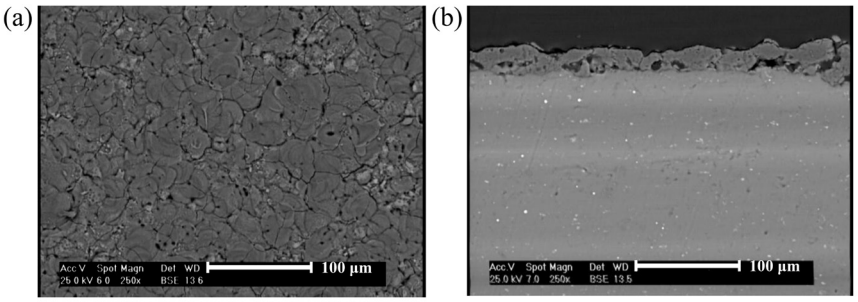

Fig. 2. SEM image of (a) surface and (b) cross-sectional area of sample 2 coated in electrolyte solution containing 2.5 g/l potash, 10 g/l sodium silicate and 8 g/l tetra sodium pyrophosphate under 500 V and duration of 10 min.

1800. Then, the samples were washed by ultrasonic method in pure ethanol and distilled water, dried in air before the PEO process.

2.2. POE process

First, the PEO coating was applied to the aluminum surface for 10 minutes at a potential of 500 V. After reaching the potential of 500 V, the current density was about 2.5 A/m^2. Then, the electric current gradually decreases during the process due to the formation of coating and its thickening.

In the pulse method, the ignition voltage is lower than the constant DC method, and due to the high intensity of the electric arcs, it is practically impossible to reach the potential of 500 V in the pulse method. Therefore, the value of electric current was considered as a controlling parameter instead of the potential value. In other words, the potential increased until the current reaches 7 A. Once this current was reached, the potential increase was stopped and kept constant during the PEO process. The electrical parameters measured during the PEO coating on the aluminum surface.

2.3. Morphological and structural studies

The phase composition of the coatings was studied by X-ray diffraction (XRD, Digaku D, max-2500) using Cu Kα radiation at 40 and 100 mA and a value of 2θ between 20° and 90°. The data was analyzed using the HighScore (Plus) v.4.7 software. For further evaluation of the morphology of the coatings and their thickness, a scanning electron microscope (Philips Model XL 30) was used. A 60-EC conductivity meter was used to measure the conductivity of the electrolyte solution. The thicknesses of the samples were measured using SEM images. Measurements were made at three points of the cross section that have the highest, lowest, and average thickness, and the average of the three values was reported. The thickness measurements were carried out using a QNix 7500 thickness gauge.

3. Results and discussion

Plasma electrolytic oxidation was performed in various electrolyte solutions and then all coated samples were cut with a micro cutter and

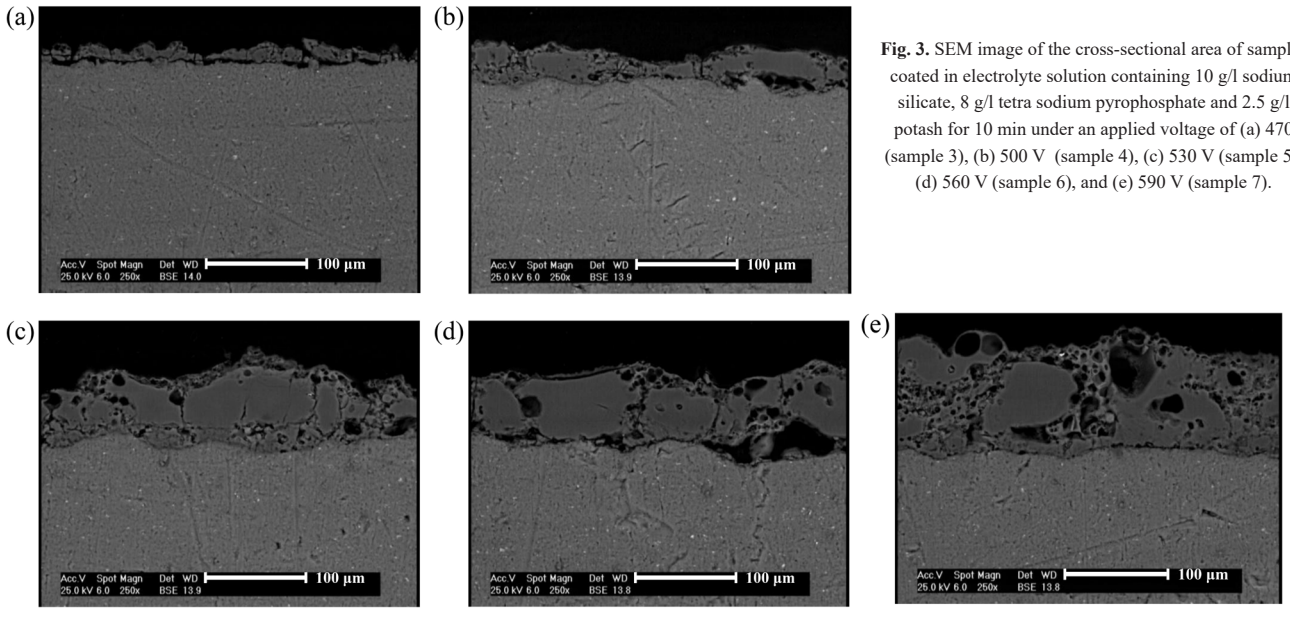

Fig. 3. SEM image of the cross-sectional area of samples coated in electrolyte solution containing 10 g/l sodium silicate, 8 g/l tetra sodium pyrophosphate and 2.5 g/l potash for 10 min under an applied voltage of (a) 470 (sample 3), (b) 500 V (sample 4), (c) 530 V (sample 5), (d) 560 V (sample 6), and (e) 590 V (sample 7).

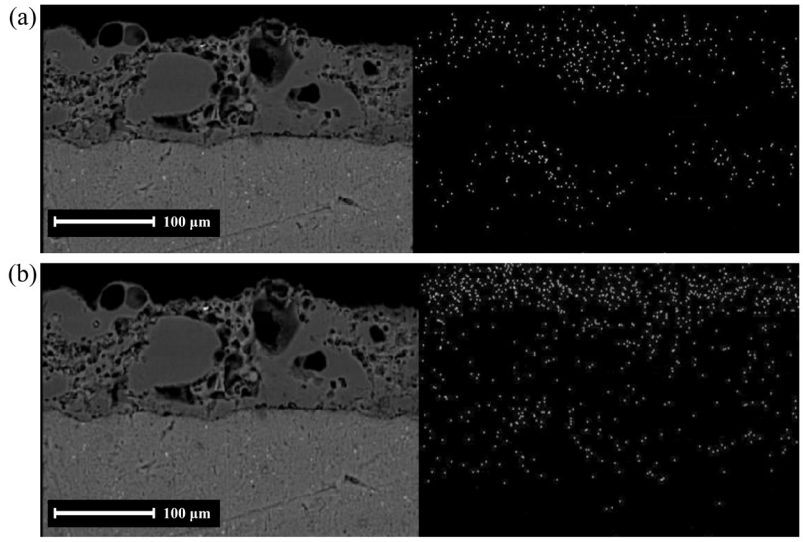

Fig. 4. Accumulation of (a) phosphorus and (b) silicon element in sample 7 coated in electrolyte solution including 10 g/l sodium silicate, 8 g/l tetra sodium pyrophosphate and 2.5 g/l potash for 10 min at an applied voltage of 590 V.

mounted to observe the surface morphology of the samples by SEM. Coated specimens generally consist of two dense layers and an outer porous layer, the structure of which is described below. At each stage, the sample with better surface properties was subjected to corrosion testing to facilitate the choice of the optimal solution.

3.1. Effect of sodium silicate on the morphology of the coating

In many studies, sodium silicate salt was used [19, 24, 27]. Therefore, to investigate the effect of this salt on the coating properties (Table 1), a sample was coated in the sodium silicate salt solution. In sample 1 that contains sodium silicate salt, the surface of the coating was so rough that it could be easily observed. As seen in Fig. 1(a), there is high volume of pores in the coating with the high thickness (about 40 mm). In addition, the volcanic structure is widely present on the surface. As seen in the cross-sectional area of the sample in Fig. 1(b), there are many holes in the interface of the coating and the substrate and consequently the coating does not adhere well to the substrate.

Because the selected solutions did not provide coating with appropriate properties, the composition of the salt solution was changed. Previous studies have suggested that tetra sodium pyrophosphate salts can be used to eliminate pores in the coatings and substrates interface, sodium aluminate to thicken coatings, and potassium hydroxide to increase solution conductivity and facilitate ion movement [19, 24]. By changing the concentration as shown in Table 3, the optimal solution is selected. Taking into account the morphology of the coating, surface properties, and the corrosion resistance, the optimal solution was sample 11. Therefore, this electrolyte composition was selected for coating.

The coating process was performed on sample 2, according to Table 1, in an electrolyte consisting of 10 g/l sodium silicate, 8 g/l tetra sodium pyrophosphate, and 2.5 g/l potassium hydroxide. The SEM images of sample 2 are seen in Fig. 2. According to SEM images, the coating surface was improved in terms of the amount and the size of micro-cavities and the structure has changed from volcanic to smooth surface. In Fig. 2(b), the cross section of the coating indicates that the sample 2 is much better than sample 1 in terms of surface morphology and the porosities were almost completely removed from the surface to the depth, but there are still cavities at the interface of the coating and the substrate that adversely affect the corrosion behavior. Fig. 2(a) clearly shows the boundaries between volcanic structures probably reduces the corrosion resistance of the coating layer.

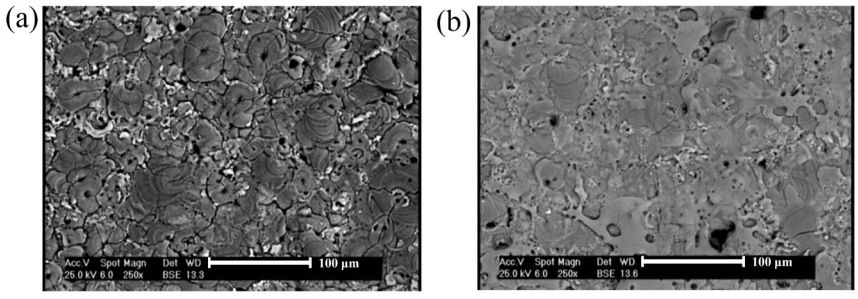

Fig. 5. SEM image of (a) sample 8 and (b) sample 9 coated in electrolyte solution including 8 g/l tetra sodium pyrophosphate 4 g/l sodium aluminate and 5 g/l potash for 10 min at an applied voltage of 500 V.

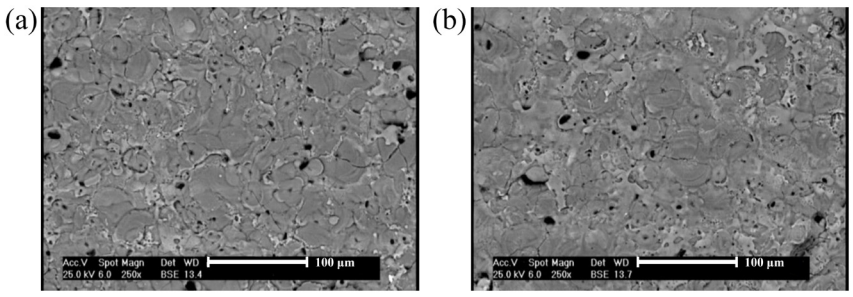

Fig. 6. SEM image of (a) sample 10 and (b) sample 11 coated in electrolyte solution consisting of 10 g/l tetra sodium pyrophosphate 3 g/l sodium aluminate and 5 g/l potash for 10 min at an applied voltage of 500 V.

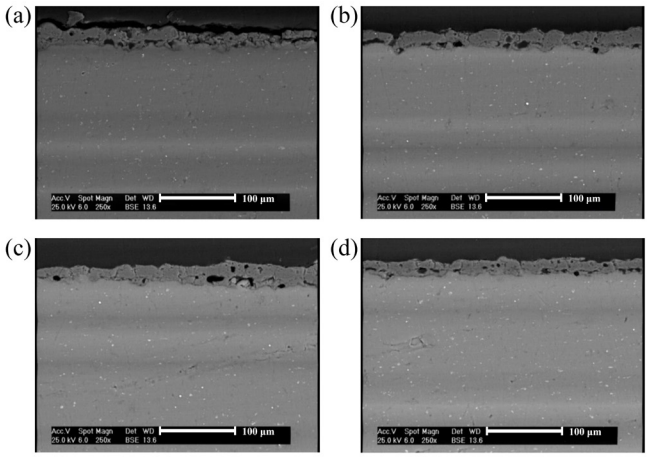

Fig. 7. SEM image of the cross section of (a) sample 8 (c) sample 10 coated in electrolyte solution including 8 g/l tetra sodium pyrophosphate 4 g/l sodium aluminate and 5 g/l potash for 10 min under an applied voltage 500 V and (b) sample 9 (d) sample 11 coated in electrolyte solution including 8 g/l tetra sodium pyrophosphate 4 g/l sodium aluminate and 3 g/l potash for 10 min at an applied voltage of 500 V.

Table 1.
Concentration of different additive electrolytes in silicate solution for coating at 500 V and 10 min at ambient temperature

Sample	KOH (g/l)	Sodium silicate (g/l)	Tetra sodium pyrophosphate (g/l)	Electrical conductivity (mS.cm^{-1})	pH
1	2.5	10	-	4.98	9.55
2	2.5	10	8	6.68	10.4

3.2. Investigation of the effect of voltage changes on the morphology of the coating prepared in silicate solution

As mentioned, the addition of tetra sodium pyrophosphate improved the surface properties; however, it was not satisfactory to be considered as an ideal coating. Thus, the effect of voltage increase on the morphology of coatings was studied. For this purpose, the coating process was performed under the conditions described in Table 2. The surface morphology of the coating was almost the same in all samples (3 to 7) and the differences were observed in the cross-sectional area. Fig. 3 corresponds to the cross-sectional area of the coated specimens under applied voltages of 470, 500, 530, 560, and 590 V. The electrolyte solution for all coated samples was the solution used for sample 2, which contains 10 g/l sodium silicate, 8g /l tetra sodium pyrophosphate, and 5 g/l potassium hydroxide. Coating process time is 10 minutes as shown in Table 2.

According to Fig. 3(a), which is related to the applied voltage of 470 V, the thickness of the coating is very low (about 18 µm). It seems that stable electric arcs have not yet been stabilized under this voltage. Also, the adhesion of the coating to the substrate is weak. In Fig. 3(b), in which the applied voltage is equal to 500 V, the coating is dense and looks uniform in terms of thickness (thickness is about 28 µm) and it has good adhesion to the substrate. The micro-cavities observed in the coating are part of the nature of plasma oxidation electrolytic coatings. In Fig. 3(c), which is related to the applied voltage of 530 V, the density

Table 2.
Different voltages applied to test the sample coated in electrolyte solution including 10 g/l sodium silicate, 8 g/l tetra sodium pyrophosphate, and 2.5 g/l potash with electrical conductivity equal to 6.68 mS.cm^{-1}and pH 10.4 in 10 min

Sample No.	3	4	5	6	7
Applied voltage (V)	470	500	530	560	590

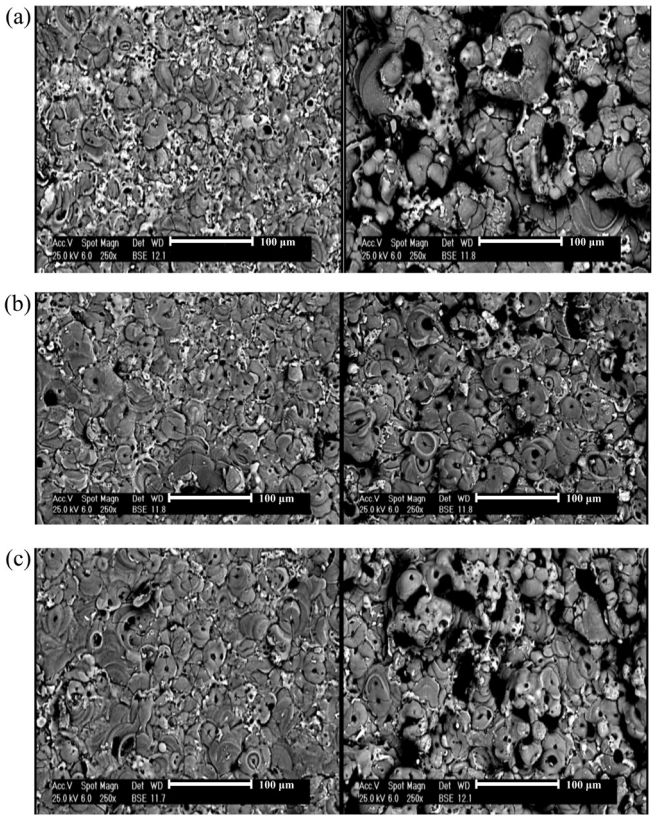

Fig. 8. Aluminum sample coated by applying a one-way pulse potential for 10 min in an electrolyte solution consisting of 10 g/l tetra sodium pyrophosphate 3 g/l sodium aluminate and 3 g/l potash at a frequency of (a) 1000Hz, (b) 2000 Hz, and (c) 3000 Hz with a working cycle of (left) 30% and (right) 70%.

of pores increased and the transverse cracks are obvious in the coating. Also, in Fig. 3(d), which is related to the voltage of 560 V, a gap was created between the coating and the substrate, and the cavities were transferred to the interface of the coating and the substrate, indicating that the coating is not suitable. In Fig. 3(e), at 590 V, the gap between the coating and the substrate is eliminated.

3.3. Dispersion map of phosphorus and silicon elements in a sample coated with silicate solution

For a more detailed study, elemental analysis was taken from sample 7 to observe the accumulation of elements on the coating as shown in Fig. 4. According to the figures, silicate has accumulated mainly on the surface, while phosphate has accumulated on the inner and outer surfaces and has low levels of phosphorus in the middle of the coating. Therefore, the use of phosphate-based compounds seems to be appropriate. On the other hand, one of the major problems of coatings is the existence of a gap between the substrate and the coating, which might be due to the supply of aluminum ions from the substrate to create the coating, which causes the transfer of this ion from the substrate/coating interface

Table 3.
Concentrations of different species to find the optimal solution under the applied voltage of 500 V in 10 minutes at ambient temperature

Sample	KOH (g/l)	sodium aluminate (g/l)	Tetra sodium pyrophosphate (g/l)	Electrical conductivity (mS.cm^{-1})	pH
8	5	4	8	11.4	10.9
9	3	4	8	10.4	10.8
10	5	3	10	13.9	10.4
11	3	3	10	12.4	10.9

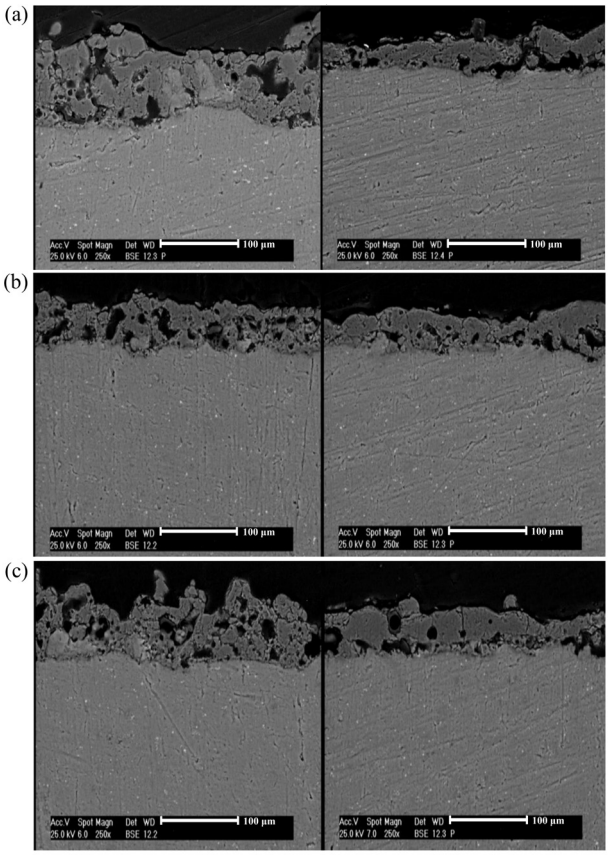

Fig. 9. Aluminum sample coated by applying a one-way pulse potential for 10 min in an electrolyte solution consisting of 10 g/l tetra sodium pyrophosphate 3 g/l sodium aluminate and 3 g/l potash at a frequency of (a) 1000 Hz, (b) 2000 Hz and (c) 3000 Hz with a working cycle of (left) 30 % and (right) 70%.

to the coating/electrolyte interface. The supply of aluminum ions in the electrolyte solution could alleviate this problem. In this way, the penetration of aluminum from the substrate is reduced and the aluminum ions in the electrolyte solution act as a contributing factor in the supply of aluminum coating and the amount of pores resulting from high transfer of aluminum from the substrate to the coating is reduced. Therefore, sodium aluminate was used in the electrolyte. In the following, different concentrations of these salts were used in order to achieve the optimal composition. It should be noted that the measured thicknesses are not real thickness values due to the porous structure of the PEO coatings.

3.4. Evaluation of the coating provided in the phosphate and silicate base electrolyte solution

As mentioned above, the use of the silicate electrolyte solution did not provide a coating with good properties; i.e. the surface generally had large pores and the coating did not adhere well to the substrate. Voltage also had little effect on coating improvement, and although the morphology appeared to be somewhat modified, it did not exhibit good corrosion resistance. However, in the case of current application regimes, the use

Table 4.
Frequency and operating cycles applied in pulse regime and with electrolyte solution electrolyte solution 10 g/l tetra sodium pyrophosphate, 3 g/l sodium aluminate, and 3 g/l potash with electrical conductivity equal to 12.45 mS.cm-1 and pH 10.9 in 10 min.

Sample	12	13	14	15	16	17
Frequency (Hz)	1000	1000	2000	2000	3000	3000
Working cycle	30%	70%	30%	70%	30%	70%

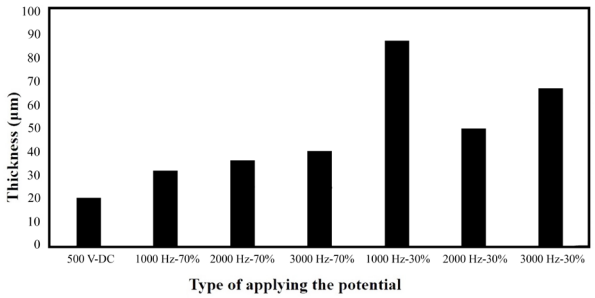

Fig. 10. The average value of coating thickness according to SEM observations under electrolyte solution including 10 g/l tetra sodium pyrophosphate 3 g/l sodium aluminate and 3 g/l potash for DC-500 V sample and Pulse samples at 1000, 2000 and 3000 frequencies in 30% and 70% duty cycle.

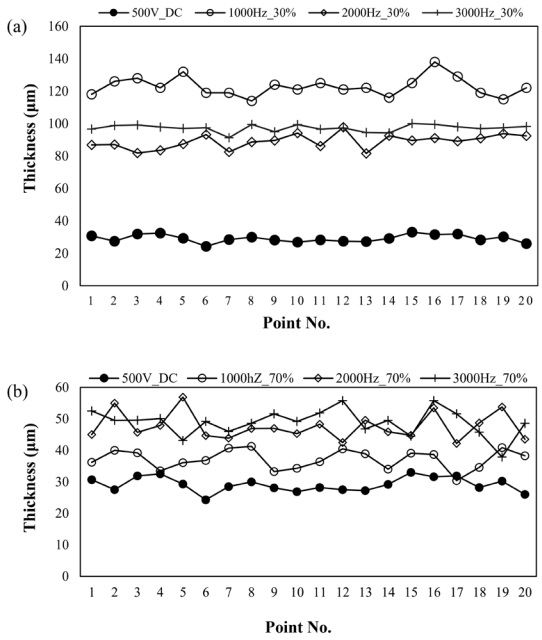

Fig. 11. Coating thicknesses in different parts of the surface under different coating conditions in electrolyte solution including 10 g/l tetra sodium pyrophosphate 3 g/l sodium aluminate and 3 g/l potash for DC-500 V sample and pulsed samples in frequency 1000, 2000 and 3000 in (a) 30% and (70%) duty cycle (measured with Quanix 7500 thickness gauge).

of this electrolyte provides excellent coatings [20]. Based on previous studies [19, 24], sodium aluminate along with sodium pyrophosphate was used in the electrolyte. Fig. 5 shows the SEM images of the surface of the coating samples in the different electrolyte salts described in Table 6. The applied voltage for all cases was 500 V, which is lower than the ignition voltage and it does not enter the intense arc zone. On the other hand, the possibility of damage to the electrolytic plasma device

Table 5.
Electrical parameters measured during the PEO process on the aluminum surface. The area of the samples was about 42 cm^2.

Parameter	500 V-DC	Duty cycle 70%			Duty cycle 30%		
		1000 Hz	2000 Hz	3000 Hz	1000 Hz	2000 Hz	3000 Hz
Breaking voltage (V)	370	341	350	359	263	280	290
Starting voltage (V)	500	414	438	452	265	291	317
Final current (A)	1.7	1	1.7	1.6	2.8	1.5	1.9

is reduced under this voltage. The test time has also been optimized in previous experiments for this electrolyte solution at 10 minutes.

In general, the morphology of the coating in the electrolytic plasma oxidation process depends on the electrical parameters and the type of solution. In sample 8 (Fig. 5(a)), the amount of porosity is very high and the pores are interconnected and many surface cracks are observed, which can be caused by a large increase in the conductivity of the solution leading to the formation of strong electric arcs on the surface of the sample. In Fig. 5(b) (sample 9), as the amount of potassium hydroxide decreased compared to sample 8, the conductivity of the solution decreased and the amount of cracks was greatly reduced. In Fig. 6 (samples 10 and 11), due to the increase in phosphate compared to samples 8 and 9, the amount of porosity has been drastically reduced. Also, in these samples, the amount of volcanic structure in the surface decreased significantly and the surfaces are very smooth. Compared to sample 10, in sample 11 (Fig. 6(b)), the amount of porosity decreased by reducing the amount of potassium hydroxide as well as the conductivity of the solution. According to the SEM results, the surface of the samples seems to provide a coating with the expected corrosion resistance.

To compare the cross sections of the specimens and the metal/coating interface, SEM images of the cross sections of each specimen were also obtained (Fig. 7). As seen in the SEM images, the electrolyte solution has a significant effect on the coating thickness and compaction. In Fig. 7(a) (sample 8), the amount of cavities and surface porosities is very high. With the decrease in the amount of potassium hydroxide in sample 9, (Fig. 7(b)), the amount of porosity is remarkably reduced. Furthermore, by increasing the amount of phosphate (Fig. 7(c), sample 10), the coating has shown a better compaction and the gap between the substrate and the coating has been reduced to a desirable level. In Fig. 7(d) (sample 11), the thickness of the coating is more uniform than that of sample 10 (Fig. 7(c)), which appears to be due to a decrease in potassium hydroxide and the uniform ignition. In general, according to the SEM evaluations, the electrolyte solution used in sample 11 was selected as the appropriate solution for PEO tests. The thickness of the coating is estimated to be about 30 μm according to the SEM images.

According to SEM images, under the same conditions of the coating time and the applied voltage, by changing the percentage of tetra sodium pyrophosphate, sodium aluminate and potassium in the electrolyte, the adhesion of coating layer to the substrate and the amount of cavities have changed, however, the thickness of coating does not show variations as indicated in Table 7.

3.5. Influence of frequency and duty cycle on pulse potential application regime

Work cycle parameters and frequency are two important and effective parameters in the pulse DC potential application regime. To evaluate the effect of the work cycle, the coating process was done in the optimal solution as described in the previous steps, i.e. electrolyte solution of sample 11 involving 10 g/l tetra sodium pyrophosphate, 3 g/l sodium aluminate and 3 g/l potassium hydroxide under 30% and 70% work cycle. Different frequencies of 1000, 2000, and 3000 Hz are also selected to investigate the effect of coating frequency. A description of the test conditions is given in Table 4. The PEO process under the DC and pulse DC potential application regimes experiences different conditions in terms of breakdown voltage, process start voltage, and final current. PEO coating can also be performed by pulse potential regimen. The voltage was applied periodically (connected and disconnected). Frequency and operating cycle are important parameters in the pulse potential application regime. In a single pulse, t_{on} and t_{off} pulse are the periods in which the current is connected and disconnected, respectively. The work cycle parameter in the pulse regime is defined as follows [24].

$$D_t = \frac{t_{on}}{t_{on}+t_{off}} \times 100 \quad (1)$$

To investigate the effect of these two coating parameters, the coating process was done in the optimal solution, i.e. electrolyte solution including 10 g/l tetra sodium pyrophosphate, 3 g/l aluminate and 3 g/l potassium hydroxide for 10 minutes. Coating is performed in 30% and 70% operating cycles at frequencies of 1000, 2000 and 3000 Hz, and the SEM images of the surface of the coating area are comparatively shown in Fig. 8. By changing the electrical parameters, the ignition behavior will change. In shorter operating cycles, micro-sparks are generated with higher density and lower intensity, which might be due to the breakdown voltage decrease, the increase in the micro-sparks distance, and the decrease in the intensity of the electrical discharge [24]. Therefore, the molten pools appearing as volcanic craters become smaller as observed in the SEM images. For example, in Fig. 8(a), which is related to the coating under the frequency of 1000 Hz, the working cycle is equal to 30% and the average diameter of the holes is about 3 μm. The micro-pores are dispersed throughout the coating layer, but in Fig. 8(a), the diameter of the pores has increased significantly (about 25 μm), and the pores are localized, and the uniform distribution of the pores was noticeably reduced.

Figs. 8 (b-c) are related to the coating at the frequencies of 2000 and 3000 Hz, respectively. With increasing the working cycle, the diameter of the pores and their percentage has increased. Also, under all three frequencies, with the increase of the work cycle, the growth of the coating becomes non-uniform and shows a mass structure which can be related to the increase in the intensity of micro-sparks due to the increase of the work cycle. The cross-sectional images are shown in Fig. 9. In Fig. 9 (a), which is related to the frequency of 1000 Hz and the duty cycle of 30%, the coating is thicker than other samples. In general, the percentage of porosity and their size have been improved compared to the DC potential application regime. In the SEM images of cross sections, spallation in the coating is observed, which seems to be related to the sample preparation for SEM observations.

3.6. Effect of thickness

The thickness of the samples was measured based on the SEM images. According to Fig. 10, the thickness of the coatings in all frequencies and operating cycles applied in the pulse mode is greater than that of the DC mode, which is probably due to the mechanism of the coating growth in the pulse mode. In the pulse mode, during the time when the voltage is cut off at the surface, the coating is dissolved and thus the coating pores are more easily filled and the coating grows more easily. Moreover, the maximum coating thickness is obtained at the frequency of 1000 Hz and the working cycle of 30%. At the same frequencies,

Table 6.
Thickness obtained from PEO coatings under different coating conditions in silicate or phosphate base electrolyte solution for 10 min

Sample	1	2	3	4	5	6	7
Thickness (μm)	112	26	18	28	75	65	97

Table 7.
Mean thickness obtained from SEM images in different amounts of tetra sodium electrophoresis of pephrophosphate, sodium aluminate and potash during coating for 10 minutes under voltage 500 V

Sample	8	9	10	11
Thickness (μm)	32	33	33	30

Table 8.
Mean thickness obtained from the thickness gauge handle in different potential application regimes

Applied regime	500 V-DC	1000 Hz-70%	2000 Hz-70%	3000 Hz-70%	1000 Hz-30%	2000 Hz-30%	3000 Hz-30%
Mean thickness (µm)	29.135	37.16	47.55	48.78	122.75	88.96	97.22

the thickness increases with decreasing duty cycle. As the duty cycle decreases, the number of micro-sparks increases and their intensity decreases. Therefore, the ignition of the coating becomes more uniform and the coating growth becomes easier. In the same work cycle, increasing or decreasing the frequency does not show a specific trend for thickness, which is probably due to the nature of PEO coating, because during coating, oxygen is constantly trapped in the coating. Furthermore, over a period in the pulse regime, which is proportional to the frequency and work cycle, the coating is dissolved and the released oxygen has the possibility to be released. However, sometimes, it may not be completely dissolved and the un-corroded areas act as centers of stress leading to the non-uniform growth of the coating in different areas.

Generally, the PEO coatings have a porous structure, and therefore, the reported thicknesses cannot be the actual thickness values. Thus, the thickness is measured at more points on the surface, but the SEM images illustrate only a limited cross section of the surface. For measuring the thickness, a QNix T500 thickness gauge was used. The results are shown in two graphs in Fig. 11. As can be seen, the thickness of the coating varies at different points on the surface. The reason for this is the nature of these coatings, which are formed based on electrical discharge and plasma generation. Due to the formation of an electric arc, molten oxide material is thrown out of the arc space and is solidified rapidly in the areas adjacent to the arc channel in contact with the electrolyte [24]. Therefore, the amount of accumulation of solid oxides in different parts of the surface will be different, which is the main cause of thickness differences in different parts of the sample surface. The strength of the electric arc and the amplitude of the created arc channel affect the amount of melt thrown out and the amount of oxides accumulated around these channels resulting in a change in the thickness of the samples and strength of arcs. The average values of the thicknesses obtained using the thickness gauge are given in Table 8.

4. Conclusions

In this research, electrolytic plasma method was used to prepare aluminum oxide coatings on the Al alloy and the effect of potential regimes was investigated. The obtained results are:

1. The optimal voltage to achieve a uniform coating with an ideal thickness and morphology was 500 V.

2. The addition of sodium silicate to the electrolyte solution caused porosity and non-adhesive coating on the substrate. On the other hand, the use of tetra sodium pyrophosphate increased the adhesion of the coating by the penetration of phosphorus into the metal/coating interface.

3. The optimal solution for coating by plasma electrolytic oxidation method is 10, 3, and 3 g/l of tetra sodium pyrophosphate, sodium aluminate, and KOH, respectively.

4. Coating by DC pulse method controls the coating process and the uniformity of the coating. The appropriate frequency for coating with pulse DC potential application regime is 1000 Hz under 30% duty cycle.

Acknowledgments

The authors received no financial support for the research, authorship and/or publication of this article.

Conflict of Interest

All authors declare no conflicts of interest in this paper.

REFERENCES

[1] V.A. Andrei, C. Radulescu, V. Malinovschi, A. Marin, E. Coaca, M. Mihalache, C.N. Mihailescu, I.D. Dulama, S. Teodorescu, I.A. Bucurica, Aluminum Oxide Ceramic Coatings on 316l Austenitic Steel Obtained by Plasma Electrolysis Oxidation Using a Pulsed Unipolar Power Supply, Coatings 10(4) (2020) 318.
[2] T. Iman, G. Ehsan, Production methods of CNT-reinforced Al matrix composites: a review, Journal of Composites and Compounds 2(2) (2020).
[3] Z. Kaiqiang, J. Ho Won, L. Quyet Van, Production methods of ceramic-reinforced Al-Li matrix composites: A review, Journal of Composites and Compounds 2(3) (2020).
[4] E.H. Jazi, R. Esalmi-Farsani, G. Borhani, F.S. Jazi, Synthesis and Characterization of In Situ Al-$Al_{13}Fe_4$-Al_2O_3-TiB_2 Nanocomposite Powder by Mechanical Alloying and Subsequent Heat Treatment, Synthesis and Reactivity in Inorganic, Metal-Organic, and Nano-Metal Chemistry 44(2) (2014) 177-184.
[5] K. Zhang, H.W. Jang, Q. Van Le, Production methods of ceramic-reinforced Al-Li matrix composites: A review, Journal of Composites and Compounds 2(3) (2020) 77-84.
[6] M. Fattahi, K. Vaferi, M. Vajdi, F. Sadegh Moghanlou, A. Sabahi Namini, M. Shahedi Asl, Aluminum nitride as an alternative ceramic for fabrication of microchannel heat exchangers: A numerical study, Ceramics International 46(8, Part B) (2020) 11647-11657.
[7] B. Nayebi, A. Bahmani, M.S. Asl, A. Rasooli, M.G. Kakroudi, M. Shokouhimehr, Characteristics of dynamically formed oxide films in aluminum–calcium foamable alloys, Journal of Alloys and Compounds 655 (2016) 433-441.
[8] A. Chlanda, P. Oberbek, M. Heljak, E. Kijeńska-Gawrońska, T. Bolek, M. Gloc, Ł. John, M. Janeta, M.J. Woźniak, Fabrication, multi-scale characterization and in-vitro evaluation of porous hybrid bioactive glass polymer-coated scaffolds for bone tissue engineering, Materials Science and Engineering: C 94 (2019) 516-523.
[9] M. Shahedi Asl, B. Nayebi, M. Shokouhimehr, TEM characterization of spark plasma sintered ZrB_2–SiC–graphene nanocomposite, Ceramics International 44(13) (2018) 15269-15273.
[10] S.A. Delbari, B. Nayebi, E. Ghasali, M. Shokouhimehr, M. Shahedi Asl, Spark plasma sintering of TiN ceramics codoped with SiC and CNT, Ceramics International 45(3) (2019) 3207-3216.
[11] V.T. Targhi, H. Omidvar, S.M.M. Hadavi, F. Sharifianjazi, Microstructure and hot corrosion behavior of hot dip siliconized coating on Ni-base superalloy IN-738LC, Materials Research Express 7(5) (2020) 056527
[12] V. Egorkin, S. Gnedenkov, S. Sinebryukhov, I. Vyaliy, A. Gnedenkov, R. Chizhikov, Increasing thickness and protective properties of PEO-coatings on aluminum alloy, Surface and coatings Technology 334 (2018) 29-42.
[13] B. Kasalica, M. Petković-Benazzouz, M. Sarvan, I. Belča, B. Maksimović, B. Misailović, Z. Popović, Mechanisms of plasma electrolytic oxidation of aluminum at the multi-hour timescales, Surface and Coatings Technology 390 (2020) 125681.
[14] T. Kikuchi, T. Taniguchi, R.O. Suzuki, S. Natsui, Fabrication of a plasma electrolytic oxidation/anodic aluminum oxide multi-layer film via one-step anodizing aluminum in ammonium carbonate, Thin Solid Films 697 (2020) 137799.
[15] S. Wang, X. Liu, X. Yin, N. Du, Influence of electrolyte components on the microstructure and growth mechanism of plasma electrolytic oxidation coatings on 1060 aluminum alloy, Surface and Coatings Technology 381 (2020) 125214.
[16] N. Angulakshmi, R.B. Dhanalakshmi, M. Kathiresan, Y. Zhou, A.M. Stephan, The suppression of lithium dendrites by a triazine-based porous organic polymer-laden PEO-based electrolyte and its application for all-solid-state lithium batteries, Materials Chemistry Frontiers 4(3) (2020) 933-940.
[17] R. Hussein, D. Northwood, X. Nie, The effect of processing parameters and substrate composition on the corrosion resistance of plasma electrolytic oxidation (PEO) coated magnesium alloys, Surface and Coatings Technology 237 (2013) 357-368.
[18] B. Ghorbanian, S.M.M. Khoie, Formation of vanadium carbide with the plasma electrolytic saturation method (PES) and comparison with Thermo Reactive diffusion method (TRD), Acta Metallurgica Slovaca 22(2) (2016) 111-119.
[19] A. Yerokhin, X. Nie, A. Leyland, A. Matthews, S. Dowey, Plasma electrolysis for surface engineering, Surface and coatings technology 122(2-3) (1999) 73-93.
[20] B. Ghorbanian, S.M.M. Khoie, M. Rasouli, R.J. Doodran, Investigation of the electrolyte effects on formation of vanadium carbide via plasma electrolytic satura-

tion method (pes), Surface Review and Letters 23(04) (2016) 1650021.
[21] Y. Gao, B. Ghorbanian, H.N. Gargari, W. Gao, Catalytic activity of char produced from brown coal for steam-gasification of bitumen oil, Petroleum Science and Technology 36(1) (2018) 75-78.
[22] Y. Gao, B. Ghorbanian, H.N. Gargari, W. Gao, Steam gasification of bitumen oil in presence of Ni/dolomite catalysts, Petroleum Science and Technology 35(21) (2017) 2074-2079.
[23] F. Momeni, B. Ghorbanian, S.M.M. Khoie, S.M.M. Nazari, M. Rasouli, Study of Current and Voltage Diagram In The Formed Vanadium Carbide Coatings Via Plasma Electrolytic Saturation Method, JOURNAL OF MATERIALS 7(11) (2016) 4073-4078.
[24] V. Dehnavi, B.L. Luan, D.W. Shoesmith, X.Y. Liu, S. Rohani, Effect of duty cycle and applied current frequency on plasma electrolytic oxidation (PEO) coating growth behavior, Surface and Coatings Technology 226 (2013) 100-107.
[25] V.T. Targhi, H. Omidvar, F. Sharifianjazi, A. Pakseresht, Hot Corrosion Behavior of Aluminized and Si-modified Aluminized Coated IN-738LC Produced by a Novel Hot-dip Process, Surfaces and Interfaces (2020) 100599.
[26] S. Rahimi, F. SharifianJazi, A. Esmaeilkhanian, M. Moradi, A.H. Safi Samghabadi, Effect of SiO_2 content on Y-TZP/Al_2O_3 ceramic-nanocomposite properties as potential dental applications, Ceramics International 46(8, Part A) (2020) 10910-10916.
[27] M. Alizadeh, M.H. Paydar, F. Sharifian Jazi, Structural evaluation and mechanical properties of nanostructured Al/B_4C composite fabricated by ARB process, Composites Part B: Engineering 44(1) (2013) 339-343.
[28] J. Curran, T. Clyne, Thermo-physical properties of plasma electrolytic oxide coatings on aluminium, Surface and Coatings Technology 199(2-3) (2005) 168-176.
[29] Y.-J. Oh, J.-I. Mun, J.-H. Kim, Effects of alloying elements on microstructure and protective properties of Al_2O_3 coatings formed on aluminum alloy substrates by plasma electrolysis, Surface and Coatings Technology 204(1-2) (2009) 141-148.